Improving the Ar I and II Branching Ratio Calibration Method: The Optical to Ultraviolet Bridge

J. E. Lawler and E. A. Den Hartog

Department of Physics, University of Wisconsin-Madison, 1150 University Ave., Madison, WI 53706; jelawler@wisc.edu, eadenhar@wisc.edu

Abstract

The Ar I and II branching ratio calibration method is discussed with the goal of improving the technique. This method of establishing a relative radiometric calibration is important in ongoing research to improve atomic transition probabilities for quantitative spectroscopy in astrophysics and other fields. Standard lamps, which produce continua, have both advantages and disadvantages as calibration sources. The problematic optical to ultraviolet (UV) bridge between a tungsten filament standard lamp in the optical and a deuterium standard lamp in the UV was discussed in earlier work on this topic [JQSRT, 207, 41]. Herein we report new measurements of key Ar II branching ratios for testing and/or improving the bridge.

1. Introduction

The preferred method for determining atomic transition probabilities or dimensionless log(*gf*) values in many complex spectra is to combine radiative lifetimes from laser induced fluorescence (LIF) measurements with branching fractions (BFs) or complete sets of branching ratios (BRs) from emission spectra as described by Den Hartog et al. [1]. Section 4 of an earlier paper by Lawler & Den Hartog [2] on this topic explored the challenge of bridging optical to ultraviolet (UV) relative radiometric calibrations based on standard lamps including a tungsten (W) filament lamp in the optical and a deuterium (D_2) lamp in the UV. In the earlier discussion it was suggested that Laser Driven Light Source (LDLS) technology might solve the bridge problem. A LDLS continuum originates from a much higher temperature than a W filament lamp, which is limited to temperatures slightly above 3000 K. Higher temperatures enhance the UV and potentially solve the bridge problem which arises from the steep roll off of W filament lamp output in the near UV. The limited overlap with D_2 standard lamps is a concern because the signal-to-noise ratio (S/N) is dropping off with the W filament lamp flux in the near UV. Some study of LDLS continuum lamps revealed that they have significant line contamination as do D_2 standard lamps at optical wavelengths above 400 nm. This prompted us to explore other alternatives for testing and/or improving the bridge.

2. Branching Ratio Calibrations

The Ar I and II branching ratio (BR) calibration method does have important advantages. It is entirely internal to the spectrum when Ar/metal hollow cathode lamps (HCLs) are used. Such HCLs provide a simple source for producing both neutral and

singly ionized spectra of almost any element. The internal calibration means that data from a high resolving power spectrometer, often a Fourier Transform Spectrometer (FTS), is recorded with the exact same optical path for the unknown, e.g. metal, spectrum and for the known calibration spectrum from Ar. This eliminates concern about window transmittance corrections, as well as effects of scattering and/or reflection of radiation inside the hollow cathode. On the other hand, standard lamps produce continua that can be used to span the gaps between Ar II and I lines. These gaps are of particular concern in the UV and infrared (IR). The coverage of Ar I and II BR calibration lines is nearly complete across the optical as tested by Wood et al. [3] but is less dense in the UV and IR. Even in the optical a steep calibration change can occur, for example if filters are used to suppress multiplex noise in FTS data. Standard lamps that produce continua are essential with narrow band interference filters.

A careful reading of Whaling et al. [4] reveals some Ar II BRs that could be used to test and/or improve the optical to UV bridge. Amongst the BRs that bridge between the optical and UV are lines from the $3s^2\ 3p^4(^1D)4p\ ^2P^o$ levels. The lines from those upper levels tend to be very strong in HCL spectra. This may be due to favorable large electron impact cross sections to the upper $3s^2\ 3p^4(^1D)4p\ ^2P^o$ levels from the ground $3s^2\ 3p^5\ ^2P^o_{3/2}$ level of Ar^+. The levels under discussion are sometimes identified as 4p' $^2P^o$ levels. Although these levels do not decay back to the ground term due to the parity rule, they do decay strongly to levels of the $3s^2\ 3p^4(^1D)4s\ ^2D$ and $3s^2\ 3p^4(^3P)4s\ ^2P$ terms. The decay of these lower levels to the ground level of the Ar^+ ion is dipole allowed and the density of Ar^+ ions is modest in most HCL sources, so significant optical depth is not expected for lines from the 4p' $^2P^o$ levels. The most valuable of these line ratios is the Ar

II (33970 cm^{-1}) / (23371 cm^{-1}) or (294.29 nm)/ (427.75 nm) BR from the 4p' $^2P^o_{3/2}$ level. Strong transitions are much less prone to blending problems than weaker transitions. The second most valuable of these ratios is the Ar II (33557 cm^{-1}) / (24196 cm^{-1}) or (297.91 nm)/ (413.17 nm) BR from the 4p' $^2P^o_{1/2}$ level. Obviously the latter is weaker, a factor of 2 just from degeneracy values, but it might be useful as a redundant check or if one or possibly both of the lines from 4p' $^2P^o_{3/2}$ level are blended with metal line(s).

3. Optical Depth Tests

Although it is not expected that the Ar II BR calibration lines will be affected by optical depth, some tests are desirable. Whaling et al. [4] states that the selected Ar I and II calibration BR values are unlikely to be affected by optical depth except for the lines of Ar I that connect to metastable lower levels. This statement is basically correct. The strongest line of the above four is the 427.75 nm line from the 4p' $^2P^o_{3/2}$ upper level. This line is only about 4 nm from the 423.72 nm line from the same upper level. This small offset means that one can compare the (427.75 nm)/(423.72 nm) BR = 0.1382 ± 1% from Whaling et al. to raw integrated line strengths from FTS data without considering changes in the relative radiometric calibration of different FTS spectra. The extensive work on rare earth atoms and ions by our University of Wisconsin (UW) team identified a list of FTS data with useful, high S/N, Ar II lines and with HCL currents ranging from 17 mA to 500 mA as summarized by Lawler et al. [5]. The relevant raw integrals were already done for the lines in question in Ar/Er HCLs by Lawler et al. [6], Ar/Gd HCLs by Den Hartog et al. [7], and Ar/Nd HCLs by Den Hartog et al. [8]. The BR value from raw integrated line strengths yield BR values quite close to the BR = 0.1382 ± 1% from Whaling et al. [4] and do not reveal any obvious current dependence

from optical depth, as shown in Table 1. Although one might argue that the current density in the HCL would be a better independent parameter than the total current, the geometry of the lamps used in recording older FTS data at the National Solar Observatory is not available. The variation in the total current covering a factor > 50 is reassuring.

Evidence that the Ar II BRs are free from optical depth errors is important but earlier measurements and calibrations of these BRs must also be tested. The (294.29 nm)/ (427.75 nm) BR = 0.6538 ± 1% and the (297.91 nm)/ (413.17 nm) BR = 0.48 ± 0% as reported in Whaling et al. [4] are the best for establishing or testing an optical to UV bridge. The first, or (294.29 nm)/ (427.75 nm) BR, was measured by various groups including: Adams &Whaling, BR = 0.67 ± 5% [9]; Danzmann & Kock, BR = 0.65 ± 2% [10]; Hashiguchi & Hasikuni, BR = 0.65 ± 4% [11]. The ± 1% uncertainty reported by Whaling et al. [4] is simply a weighted standard deviation of the above measurements. The second, or (297.91 nm)/ (413.17 nm) BR, was measured by various groups including: Adams & Whaling, BR = 0.48 ± 5% [9]; Danzmann & Kock, BR = 0.48 ± 2% [10]; Hashiguchi & Hasikuni, BR = 0.49 ± 3% [11]. Again, the ± 0% uncertainty reported by Whaling et al. [4] indicates the agreement of the above measurements excluding the measurement from Japan is better than ±0.5%. Calibration methods crossing the optical to UV bridge are clearly critical to all of these measurements. Adams &Whaling [9] and Danzmann & Kock [10] calibrated using Fe I measurements by the Oxford group (Blackwell et al. [12-15]). The Fe I absorption measurements by the Oxford group are arguably the best relative log(*gf*) measurements available, with reported uncertainties of ≤ ± 1%. Unfortunately no other team has made a similar large set of

measurements on Fe I with comparably small uncertainties. The small ± 1% uncertainties on the relative log(*gf*) values from the Oxford group must be regarded as unconfirmed. Hashiguchi & Hasikuni [11] used standard lamps and unfortunately they do not discuss the optical to UV bridge needed between a W filament standard lamp calibration in the optical and D_2 standard lamp calibration in the UV. There is a clear need for an independent test of the key BRs needed to test or improve the optical to UV bridge between a W filament calibration in the optical and a D_2 standard lamp calibration in the UV.

4. New Measurements of Bridge Branching Ratios

Primary optical and near UV radiometric standards have evolved in the last few decades from source standards to detector standards. The High Accuracy Cryogenic Radiometer (HACR) as described by Gentile et al. [16] is now the primary U.S. standard for radiometric measurements in the optical and near UV. The use of built-in calibration resistors enables one to tie radiometric measurements back to fundamental (e.g. quantum Hall effect) electrical standards. Detectors such as Si photodiodes (PDs) are used to transfer radiometric calibrations from the HACR at the National Institute of Standards and Technology (NIST) to other labs. The 2σ uncertainty of the Spectral Power Responsivity of a NIST calibrated Si PD typically varies from about 1% in the UV longer than 220 nm to about 0.2% in the optical. The stability of a PD is better than that of standard lamps. It is thus logical to use a NIST calibrated Si PD to test and possibly improve the key Ar BRs.

One way to use a NIST calibrated Si PD for BR measurements is to calibrate a spectrometer and then use the spectrometer to measure BRs. Transferring the Si PD

calibration to a spectrometer can be accomplished using a stable lamp and a set of multilayer dielectric (MLD) filters, preferably in a filter wheel. Our first attempt using a Xe arc lamp for such a calibration transfer was not successful because the Xe arc lamp did not have the needed stability. Mercury pen lamps have better stability than Xe arc lamps and have been calibrated at NIST as low accuracy irradiance standards by Reader et al. [17]. The fact that Hg Pen Lamps are line, instead of continua, sources has an advantage in that it is not necessary to map the various filter transmissions as a function of wavelength. One only needs to establish that the filter isolates a specific line or set of lines and establish that the filter transmits enough flux so that a good power measurement can be made using the NIST calibrated Si PD. Although strong Hg I lines are widely spaced across the optical and UV, they can still be used for a calibration of a spectrometer with a slowly changing spectral response which in our study also has a modest limit of resolution. The fact that some strong Hg I lines fall near the proposed Ar II BR calibration lines is an important, admittedly fortuitous, advantage. The instrument of choice was a 0.5 m focal length Jarrell Ash spectrometer with a 1180 groove/mm diffraction grating blazed at 250 nm and with a 1024 element photodiode array (PDA).

Figure 1 is a schematic of the optical set up for the Ar II BR measurements. The radiation from the Hg Pen Lamp is collimated and sent through a MLD filter that isolates a single line or set of Hg I lines. Lenses used for collimation are not shown. A monochromatic real image of the Pen Lamp is formed ~ 30 cm in front of the entrance slit of the spectrometer. The Hg Pen Lamps are best used as irradiance standards because there is a radial dependence of the flux from the lamp tube that varies with excitation energy of the upper radiating level. This type of structure makes it very difficult to use

such a lamp as a radiance standard. The real image of the lamp some distance from the entrance slit of the spectrometer results in use of only the center of the mirrors and grating of the spectrometer. Such component illumination effects are a source of a small additional systematic uncertainty in our measurements. The monochromatic radiation from the Hg Pen Lamp transmitted by the MLD filter is sufficient for direct measurement with the NIST calibrated Si PD with satisfactory S/N. The monochromatic real image of the pen lamp is formed using the same spherical mirror to focus radiation from a See-Through HCL onto the entrance slit of the spectrometer. The Ar/Sc See-through HCL is used to facilitate window transmittance measurements.

Figure 2 is a plot of four separate calibrations of the relative radiometric response of the 0.5 m focal length Jarrell Ash grating spectrometer with the PDA detector. Each calibration was taken on a different day for a different set of Ar II BR measurements. It is fortuitous that the most important Ar II transitions at 427.75 nm and 294.29 nm, indicated by vertical lines in the figure, are near Hg I calibration transitions at 435.83 nm and 296.73 nm. The relatively weak wavelength dependence of the response of the spectrometer and PDA is due in part to the use of a grating blazed for 250 nm.

Any wavelength dependent variations in the HCL window transmittance do affect BR measurements with either standard lamp or standard detector calibrations of the spectrometer. Such variations from an imperfect window polish and from the growth of a sputtered metal film can be significantly larger than the variations due to Fresnel reflections, which are easily computed from the known index of refraction of the window material. One of the advantages of the See-Through HCL is the combined transmittance of the back and front window can be measured without sacrificing a sealed commercial

lamp. Figure 3 is a plot of the wavelength dependence of the square root of the combined front and back window transmittance. An assumption of perfect symmetry between the front and back window is essential if one is to use the square root of the combined transmittance. The location of the anode in the See-Through Sc/Ar HCL used in this study breaks the symmetry of the lamp. The correction for transmittance, which strengthens the UV BR in comparison to the visible BR = 1, is made larger by this asymmetry. Assuming perfect symmetry, the correction is 1.032 from the data of Figure 3. There is evidence that the sputtered metal film produced higher losses in the transmittance of the front window near the anode and resulted in a correction of 1.050. The upper limit on this correction assuming the back window has only Fresnel reflection losses is 1.059. The expanded scale suggests that the correction from the wavelength dependent window transmission loss is substantial, but it is actually rather small and the systematic uncertainty in the most important Ar II BR from the window transmittance correction is ~ ±1% or less.

5. Comparison to Earlier Ar II Branching Ratio Measurements

Table 2 (a) includes measurements of the Ar II BR (294.29 nm)/ (427.75 nm) from this experiment and from other published experiments, and 2(b) includes measurements of the Ar II BR (297.91 nm)/ (413.17 nm) from this experiment and from other published experiments. It is likely that all uncertainties in Table 2 are single σ standard deviation statistical scatter uncertainties. Systematic uncertainties are often quite difficult to estimate and could be larger than the statistical scatter. The difference between the Hg Pen Lamp illumination and the HCL illumination of the spectrometer mirrors and gratings is mentioned above as a possible source of systematic error in this experiment.

The admittedly fortuitous near match of Ar II and Hg I lines results in, at most, a small systematic uncertainty from the linear interpolation, $\leq \pm 1\%$. The older measurements in Table 2 also have systematic uncertainty, but from different sources. The $\leq \pm 1\%$ accuracy and precision of the relative Fe I log(*gf*)s from Oxford can neither be confirmed or disputed based on our new measurements. The Hannover group [18, 19] pointed out that Blackwell et al. [12-15] omitted effects of diffusion in modeling their oven and that this omission may have resulted in an effective temperature error. Bard et al. [19] also expressed concerns about the Fe vapor pressure curve. However, there is no evidence at this time that the Blackwell et al. [12-15] data have errors typically larger than ±1%. The differences in potential systematic errors between the BR measurements of this work calibrated using standard detector and earlier measurements calibrated using standard source does provide a significant new test of the Ar I and II BR calibration method and supports the use of selected Ar II BRs for testing and/or establishing a reliable optical to UV bridge.

6. Summary

The troublesome bridge between a relative radiometric calibration in the optical from a W filament standard lamp and a relative radiometric calibration in the UV from a D_2 lamp may be tested and/or improved using carefully selected Ar II BRs. The best Ar II BRs are for lines from the 4p' $^2P_{3/2}$ and 4p' $^2P_{1/2}$ levels of Ar^+. Those selected BRs are re-measured in our experiment using a calibrated detector for the first time. Any possible systematic effects in earlier measurements and in our new measurements should be different, and appear to be smaller than random statistical effects.

ACKNOWLEDGEMENTS

This research is supported by NASA grant NNX16AE96G and NSF grants AST-1516182 and AST-1814512.

FIGURE CAPTIONS

Figure 1: Schematic of the experiment. Photo Diode is abbreviated as PD and Photo Diode Array, the detector on the spectrometer, is abbreviated as PDA.

Figure 2: Plot of four separate calibrations of the relative radiometric response of the 0.5 m Jarrell Ash spectrometer and PDA from the Spectral Power Responsivity of the NIST calibrated Si photodiode. The vertical lines at 294.29 nm and 427.75 nm indicate the location of the most important Ar II lines.

Figure 3: The upper curve with "x" symbols is the single fused silica window transmittance computed from the tabulated index of refraction of fused silica including only Fresnel reflection losses. The lower curve with the solid triangles and very small error bars is the square root of the two-window measured transmittance. This curve is a single window transmittance assuming the front and back windows of the HCL are identical. The vertical lines at 294.29 nm and 427.75 nm indicate the location of the most important Ar II transitions.

REFERENCES

[1] Den Hartog, E. A., Lawler, J. E., Sobeck, J. S., Sneden, C., & Cowan, J. J. 2011, ApJS, 194, 35

[2] Lawler, J. E., & Den Hartog E. A. 2018, JQSRT, 207, 41

[3] Wood, M. P., Sneden, C., Lawler, J. E., et al. 2018, ApJS, 234, 25

[4] Whaling, W., Carle, M. T., & Pitt, M. L. 1993, JQSRT, 50, 7

[5] Lawler, J. E., Sneden, C., Cowan, J. J., Ivans, I. I., & Den Hartog, E. A. 2009, ApJS, 182, 51

[6] Lawler, J. E., Sneden, C., Cowan, J. J., Wyart, J.-F., Ivans, I. I., Sobeck, J. S., Stockett, M. H., & Den Hartog, E. A. 2008, ApJS, 178, 71.

[7] Den Hartog, E. A. Lawler, J. E., Sneden, C. & Cowan, J.J. 2006, ApJS, 167, 292.

[8] Den Hartog, E. A. Lawler, J. E., Sneden, C. & Cowan, J.J. 2003, ApJS, 148, 543.

[9] Adams, D. L., & Whaling, W. 1981, JOSA, 71, 1036

[10] Danzmann, K., & Kock, M. 1982, JOSA, 72, 1556

[11] Hashiguchi, S., & Hasikuni, M. 1985, JPSJ, 54, 1290

[12] Blackwell, D. E., Ibbetson P. A., Petford, A. D., & Shallis M. J. 1979a, MNRAS, 186, 633

[13] Blackwell, D. E., Petford, A. D., & Shallis M. J. 1979b, MNRAS, 186, 657

[14] Blackwell, D. E., Petford, A. D., Shallis M. J., & Simmons, G. J. 1980, MNRAS, 191, 445

[15] Blackwell, D. E., Petford, A. D., Shallis M. J., & Simmons, G. J. 1982, MNRAS, 199, 43

[16] Gentile, T. R., Houston, J. M., Hardis, J. E., Cromer, C. L., & Parr A. C. 1996, Appl.

Opt., 35, 1056

[17] Reader, J., Sansonetti, C. J. & Bridges, J. M. 1996, Appl. Opt. 35, 78

[18] Bard, A., & Kock, M.1994, A&A, 282, 1014

[19] Bard A., Kock A., & Kock, M. 1991, A&A, 248, 315

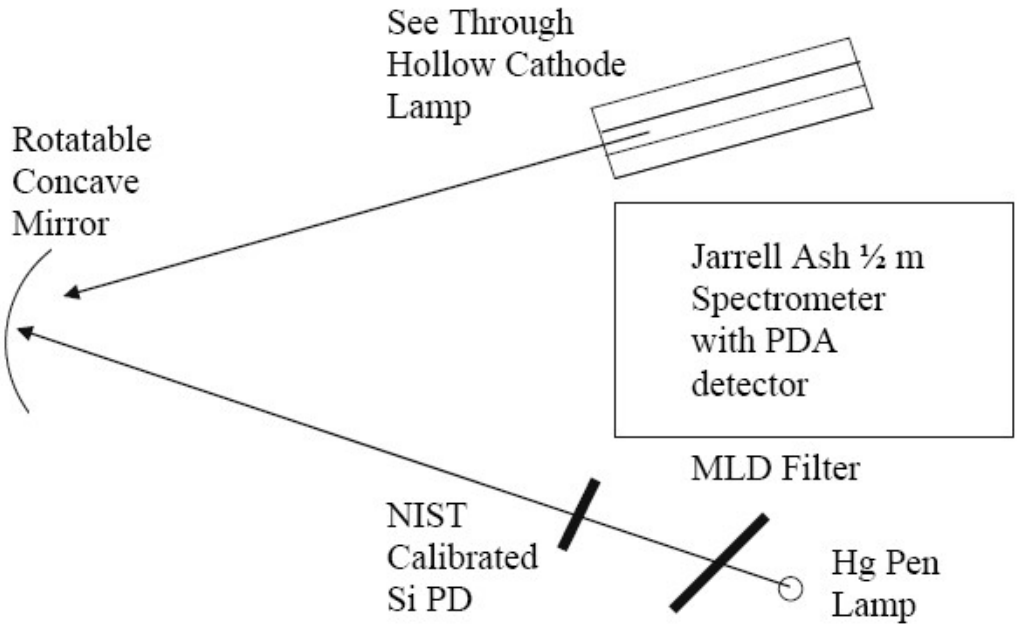

Figure 1. Schematic of the experiment. Photo Diode is abbreviated as PD and Photo Diode Array, the detector on the spectrometer, is abbreviated as PDA.

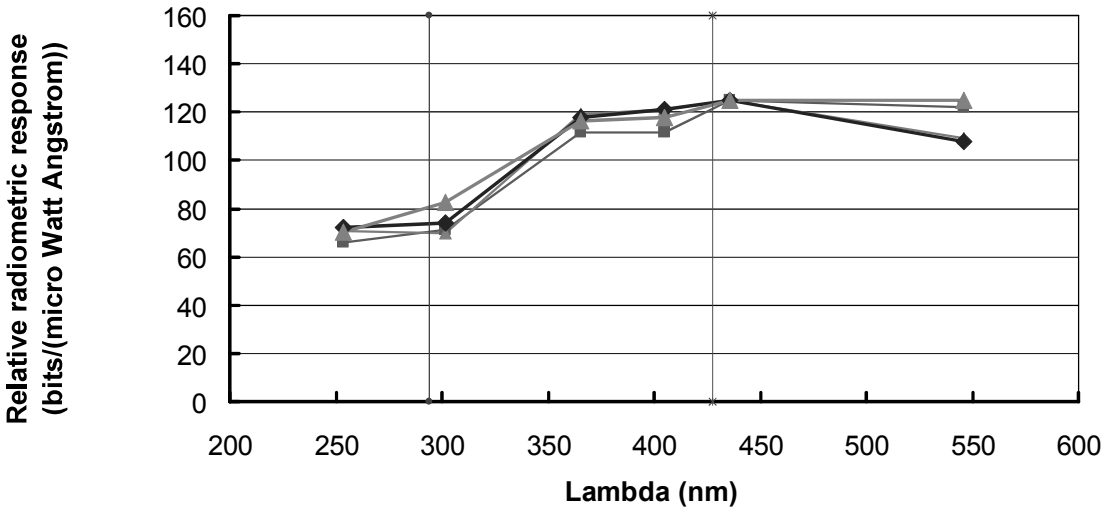

Figure 2: Plot of four separate calibrations of the relative radiometric response of the 0.5 m Jarrell Ash spectrometer and PDA from the Spectral Power Responsivity of the NIST calibrated Si photodiode. The vertical lines at 294.29 nm and 427.75 nm indicate the location of the most important Ar II lines.

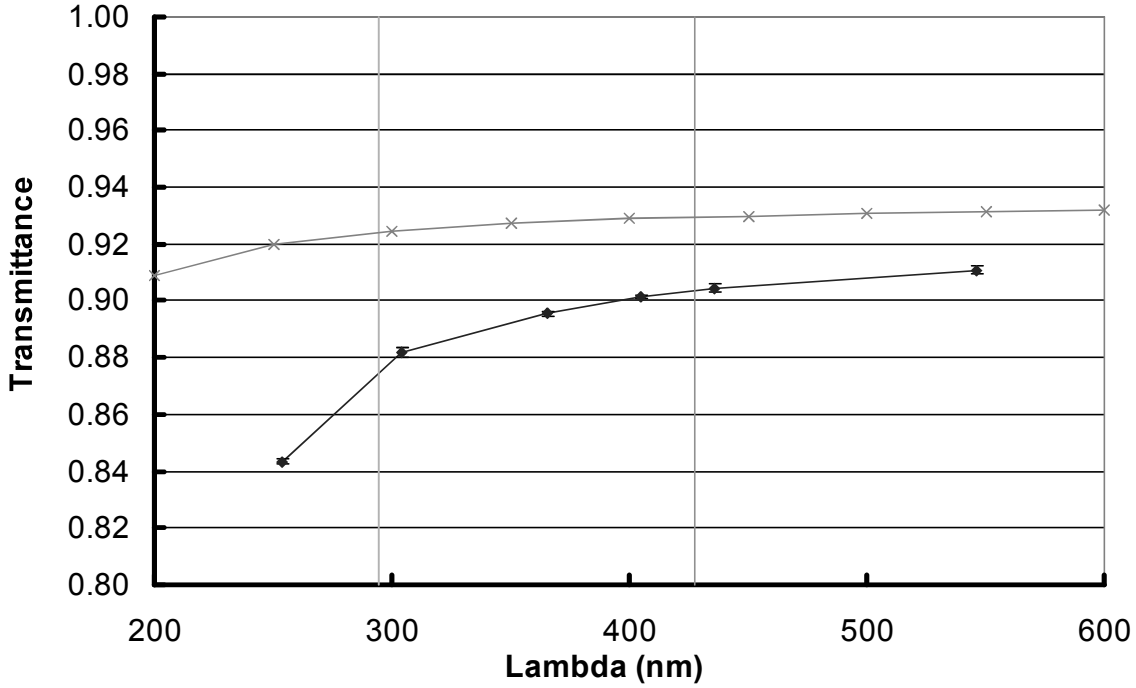

Figure 3: The upper curve with "x" symbols is the single fused silica window transmittance computed from the tabulated index of refraction of fused silica including only Fresnel reflection losses. The lower curve with the solid triangles and very small error bars is the square root of the two-window measured transmittance. This curve is a single window transmittance assuming the front and back windows of the HCL are identical. The vertical lines at 294.29 nm and 427.75 nm indicate the location of the most important Ar II transitions.

Table 1: Optical depth test on the Ar II line at 427.75 nm or 23371.4 cm^{-1}.

Er

Sp	423.72 nm 23593.7 cm^{-1} raw integral	S/N	427.75 nm 23371.4 cm^{-1} raw integral	S/N	raw ratio	Lamp Current (mA)	Beam Splitter	Filter	Detector
1	3725364	30	27759270	65	0.1342	500.0	UV		SB Si diode
2	7611321	30	57133000	60	0.1332	500.0	UV	CuSO4	SB Si diode
3	2241559	40	18299930	40	0.1225	500.0	VIS		SB Si diode
4	3765796	20	30550876	40	0.1233	500.0	VIS		SB Si diode
5	298004.4	8	2352906	50	0.1267	300.0	VIS		SB Si diode
7	31900954	30	2.37E+08	70	0.1347	26.5	UV		SB Si diode
8	15536378	40	1.17E+08	90	0.1330	27.0	UV		SB Si diode
9	8978791	40	67617096	90	0.1328	26.5	UV		SB Si diode
10	2009929	35	14977252	80	0.1342	23.0	UV		SB Si diode
11	1252667	30	9659962	80	0.1297	17.0	UV		SB Si diode
	Mean ± Standard Deviation				0.1304 ± .0047				

Gd

Sp	423.72 nm 23593.7 cm^{-1} raw integral	S/N	427.75 nm 23371.4 cm^{-1} raw integral	S/N	raw ratio	Lamp Current (mA)	Beam Splitter	Filter	Detector
1	10677720	100	78794272	200	0.1355	26.0	UV		SB Si diode
2	4703596	100	35143812	200	0.1338	23.0	UV		SB Si diode
3	20275116	100	1.5E+08	200	0.1352	30.0	UV		SB Si diode
4	6130528	100	46250116	200	0.1326	15.0	UV		SB Si diode
5	4040156	100	30751254	200	0.1314	12.5	UV		SB Si diode
6	695321.4	100	5271743	200	0.1319	295.0	UV	CuSO4	SB Si diode
7	708828.9	100	5355397	200	0.1324	290.0	UV	CuSO4	SB Si diode
	Mean ± Standard Deviation				0.1333 ± 0.0016				

Nd

Sp	423.72 nm 23593.7 cm^{-1} raw	S/N	427.75 nm 23371.4 cm^{-1} raw	S/N	raw ratio	Lamp Current (mA)	Beam Splitter	Filter	Detector

	integral		integral						
1	55295900	90	4.11E+08	200	0.1346	26.0	UV		SB Si diode
2	58244988	90	4.32E+08	200	0.1350	26.0	UV		SB Si diode
3	3331897	90	24964508	200	0.1335	21.5	UV		SB Si diode
4	2785030	90	20619584	200	0.1351	18.5	UV		SB Si diode
5	6317856	50	44657120	200	0.1415	300.0	UV	WG-5 @ 10deg	Large Si diode
6	5858684	40	40356004	200	0.1452	300.0	UV	WG-5 @ 10deg	Large Si diode

0.1375 ± 0.0047

Mean ± Standard Deviation

Table 2. (a) Measurements on the Ar II (33970 cm^{-1}) / (23371 cm^{-1}) or (294.29 nm)/ (427.75 nm) BR from this experiment and from other published experiments. (b) Similar measurements of the Ar II (33557 cm^{-1}) / (24196 cm^{-1}) or (297.91 nm)/ (413.17 nm) BR.

(a)	BR	% uncertainty
Adams & Whaling (1981) with Oxford Fe I calibration	0.67	5
Danzman & Kock (1982) with Oxford Fe I calibration	0.65	2
HashiguchI & Hasikuni (1985) with standard lamps	0.65	4
This Experiment with a NIST calibrated Si photodiode	0.630	2.8
Weighted Mean	0.646	1.4

(b)	BR	% uncertainty
Adams & Whaling (1981) with Oxford Fe I calibration	0.48	5
Danzman & Kock (1982) with Oxford Fe I calibration	0.48	2
HashiguchI & Hasikuni (1985) with standard lamps	0.49	3
This Experiment with a NIST calibrated Si photodiode	0.484	6.9
Weighted Mean	0.483	1.5